Tunneling through nanosystems: Combining broadening with many-particle states

Jonas Nyvold Pedersen and Andreas Wacker
Department of Physics, University of Lund, Box 118, 22100 Lund, Sweden
(Received 5 July 2005; revised manuscript received 1 September 2005; published 21 November 2005)

We suggest an approach for transport through finite systems based on the Liouville equation. By working in a basis of many-particle states for the finite system, Coulomb interactions are taken fully into account and correlated transitions by up to two different contact states are included. This latter extends standard rate equation models by including level-broadening effects. The main result of the paper is a general expression for the elements of the density matrix of the finite size system, which can be applied whenever the eigenstates and the couplings to the leads are known. The approach works for arbitrary bias and for temperatures above the Kondo temperature. We apply the approach to standard models and good agreement with other methods in their respective regime of validity is found.

DOI: 10.1103/PhysRevB.72.195330 PACS number(s): 73.23.Hk, 73.63.−b

I. INTRODUCTION

Transport through nanosystems such as quantum dots and molecules has received enormous interest within the last decade.[1–3] Typically this problem is treated within one of the two following different approximations: (i) Rate equations[4] for electrons entering and leaving the system, which can also take into account complex many-particle states in the central region.[5,6] Here broadening effects of the levels are entirely neglected. It can be shown that these rate equations become exact in the limit of high bias.[7] (ii) The transmission formalism, which is usually evaluated by Green function techniques[8,9] (alternatively, scattering states can be calculated directly[10]), allows for a consistent treatment of level broadening due to the coupling to the contacts. In principle, many-particle effects can be incorporated into this formalism, but the determination of the appropriate self-energies is a difficult task, where no general scheme has been found by now. Thus, many-particle effects are usually considered on a mean-field basis including exchange and correlation potentials,[11–14] which are of particular importance for the transport through molecules. Mean-field calculations are well justified for extended systems, such as double-barrier tunneling diodes,[15,16] which exhibit many degrees of freedom (e.g., in the plane perpendicular to the transport). However, the bistability frequently obtained for such structures is questionable for systems with very few degrees of freedom as studied here. See, e.g., the discussion in Sec. III B 4 of Ref. 17.

In our paper we want to bridge the gap between these approaches by considering the Liouville equation for the dynamics of the central region coupled to the contacts. The approach works within a basis of arbitrary many-particle states, thus fully taking into account the interactions within the central region. While the first order in the coupling reproduces previous work using rate equations,[18] the second order consistently takes into account broadening effects. This is analogous to the consistent treatment of broadening for tunneling resonances in density-matrix theory.[19]

The paper is organized as follows: We first present the formalism in Sec. II. Then we demonstrate its application to the simple problem of tunneling through a single level, Sec. III. We show explicitly that the exact Green function result is recovered for all biases and temperatures. In Sec. IV we give results for the double-dot system with Coulomb interaction where both standard approaches fail. Finally we consider the spin-degenerate single dot in Sec. V to investigate Coulomb blockade as well as the limit of low temperatures.

II. INTRODUCING THE FORMALISM

The total Hamiltonian for the system consisting of leads and the dot can be written as

$$H = H_D + H_{\text{Leads}} + H_T. \tag{1}$$

The first term describes the dot. Our key issue is the assumption that the dot can be diagonalized in absence of coupling, and the (many-particle) eigenstates and eigenenergies for H_D are denoted $|a\rangle$ and E_a. Thus we have

$$H_D = \sum_a E_a |a\rangle\langle a|. \tag{2}$$

The leads are described by free-particle states

$$H_{\text{Leads}} = \sum_{k\sigma\ell} E_{k\sigma\ell} c^\dagger_{k\sigma\ell} c_{k\sigma\ell} \tag{3}$$

where $\sigma = \uparrow, \downarrow$ describes the spin, k labels the spatial wave functions of the contact states and ℓ denotes the lead. In the following we assume two leads, i.e., $\ell = L, R$, but generalization to more leads is straightforward. Finally, the last part in the Hamiltonian expresses the tunneling between the states in the leads and the dot

$$H_T = \sum_{k\sigma\ell, ab} [T_{ba}(k\sigma\ell)|b\rangle\langle a| c_{k\sigma\ell} + c^\dagger_{k\sigma\ell}|a\rangle\langle b| T^*_{ba}(k\sigma\ell)]. \tag{4}$$

The matrix element $T_{ba}(k\sigma\ell)$ is the scattering amplitude for an electron in the state $k\sigma\ell$ tunneling from the lead onto the dot, thereby changing the dot state from state $|a\rangle$ to a state $|b\rangle$. Their evaluation is sketched in Appendix A. Note that this amplitude vanishes unless the number of electrons in state $|b\rangle$, N_b, equals $N_a + 1$. We will generally denote states

such that the particle number increases with the position in the alphabet of the denoting letter.

Before proceeding it is important to introduce a consistent notation in order to keep track of the many-particle states in the leads. A general state vector for the entire system is written as $|ag\rangle = |a\rangle \otimes |g\rangle$, with $|g\rangle = |\{N_{k\ell\sigma}\}\rangle$ denoting the state of both leads where $N_{k\sigma\ell} \in \{0,1\}$. Throughout the derivation of the general equations we use the following notation to ensure the anticommutator rules of the operators

(i) $|g - k\sigma\ell\rangle \equiv c_{k\sigma\ell}|g\rangle$ and $|g + k\sigma\ell\rangle \equiv c^\dagger_{k\sigma\ell}|g\rangle$. That is, $|g - k\sigma\ell\rangle$ denotes the same set of indices as the state $|g\rangle$, but with $N_{k\sigma\ell}$ reduced by one. Furthermore it contains a minus sign depending on the number of occupied states to the left of the position $k\sigma\ell$.

(ii) $|gk\sigma\ell\rangle \equiv c^\dagger_{k\sigma\ell}c_{k\sigma\ell}|g\rangle$ and $|g\overline{k\sigma\ell}\rangle \equiv c_{k\sigma\ell}c^\dagger_{k\sigma\ell}|g\rangle$. That is, $|gk\sigma\ell\rangle = \delta_{N_{k\sigma\ell},1}|g\rangle$.

(iii) The order of indices is opposite to the order of the operators. For example, $|g - k'\sigma'\ell' + k\sigma\ell\rangle = c^\dagger_{k\sigma\ell}c_{k'\sigma'\ell'}|g\rangle = -c_{k'\sigma'\ell'}c^\dagger_{k\sigma\ell}|g\rangle = -|g + k\sigma\ell - k'\sigma'\ell'\rangle$ for $k\sigma\ell \neq k'\sigma'\ell'$, which is tacitly assumed, unless stated otherwise.

To simplify the notation, $\sigma\ell$ is only attached to k the first time the index k appears in the equation, and in the following it is implicitly assumed to be connected with k. We also use the convention that $\Sigma_{k\sigma(\ell)}$ means summing over k and σ with a fixed ℓ, which is being connected to k in this sum.

The matrix elements of the density operator $\hat{\rho}$ are denoted $\rho_{ag;bg'} = \langle ag|\hat{\rho}|bg'\rangle$ and the time evolution of the matrix elements are governed by the von Neumann equation

$$i\hbar\frac{d}{dt}\rho_{ag;bg'} = \langle ag|H\hat{\rho} - \hat{\rho}H|bg'\rangle \tag{5}$$

The particle current from the left lead into the structure, J_L, equals the rate of change in the occupation of the left lead. We find that

$$\begin{aligned} J_L &= -\frac{d}{dt}\sum_{k\sigma(L)}\langle c^\dagger_k c_k\rangle \\ &= -\frac{d}{dt}\sum_{k\sigma(L)}\rho_{bg,bgk} = -\frac{2}{\hbar}\sum_{k\sigma(L),cb}\mathrm{Im}\left\{\sum_g T^*_{cb}(k)\rho_{cg-k;bg}\right\}, \end{aligned} \tag{6}$$

where we have used the definition of the density operator to calculate the average value of the number operator in the left lead.

The goal is to determine these elements of the density matrix, which describe the correlations between the leads and the dot. They are determined using the equation-of-motion technique, and from Eq. (5) we obtain

$$\begin{aligned} i\hbar\frac{d}{dt}&\rho_{cg-k\sigma\ell;bg} \\ &= (E_c - E_b - E_k)\rho_{cg-k;bg} + \sum_{b'} T_{cb'}(k)\rho_{b'gk;bg} \\ &- \sum_{c'}\rho_{cg-k;c'g-k}T_{c'b}(k) + \sum_{k'\sigma'\ell'}\left(\sum_{b'} T_{cb'}(k')\rho_{b'g-k+k';bg}\right. \\ &+ \sum_d T^*_{dc}(k')\rho_{dg-k-k';bg} - \sum_{c'}\rho_{cg-k;c'g-k'}T_{c'b}(k') \\ &\left. - \sum_a \rho_{cg-k;ag+k'}T^*_{ba}(k')\right). \end{aligned} \tag{7}$$

While $\rho_{cg-k\sigma\ell;bg}$ describes the transition of an electron with quantum number k and spin σ from lead ℓ to the central region, terms like $\rho_{b'g-k+k';bg}$ describe the correlated transition of two electrons with k and k'. $\rho_{b'g-k+k';bg}$ satisfies a similar equation of motion containing also correlated transition of three electrons on the right-hand side. In order to break the hierarchy we apply three approximations.

(i) We only consider coherent processes involving transitions of at most two different k-states. (ii) The time dependence of terms generating two-electron transition processes is neglected, which corresponds to the Markov limit.[20] (iii) We assume that the level occupations $f_{k\sigma\ell}$ in the leads are unaffected by the kinetics of the dot, so it is possible to factorize the density in the leads and on the dot. This is realistic for "large" leads which are strongly coupled to reservoirs, i.e., good contacts.

Defining

$$w_{b'b} = \sum_g \rho_{b'g;bg}, \tag{8}$$

$$\phi_{ba}(k\sigma\ell) = \sum_g \rho_{bg-k;ag} \tag{9}$$

we find the following set of coupled differential equations (see Appendix B for a detailed derivation):

$$\begin{aligned} i\hbar\frac{d}{dt}\phi_{cb}(k\sigma\ell) &= (E_c - E_b - E_k)\phi_{cb}(k) + \sum_{b'} T_{cb'}(k)f_k w_{b'b} - \sum_{c'}(1 - f_k)w_{cc'}T_{c'b}(k) \\ &+ \sum_{a,b',k'\sigma'\ell'}\frac{[T_{cb'}(k')f_{k'}\phi_{b'a}(k) - (1 - f_k)\phi_{cb'}(k')T_{b'a}(k)]T^*_{ba}(k')}{E_k + E_{k'} - (E_c - E_a) + i0^+} \\ &+ \sum_{a,b',k'\sigma'\ell'}\frac{[(1 - f_{k'})\phi_{cb'}(k)T_{b'a}(k') - T_{cb'}(k)f_k\phi_{b'a}(k')]T^*_{ba}(k')}{E_k + E_{k'} - (E_c - E_a) + i0^+} \end{aligned}$$

$$+\sum_{a,b',k'\sigma'\ell'}\frac{T_{cb'}(k')[f_{k'}\phi_{b'a}(k)T^*_{ba}(k')-T_{b'a}(k)f_k\phi^*_{ba}(k')]}{E_k-E_{k'}-(E_{b'}-E_b)+i0^+}$$

$$+\sum_{b',c',k'\sigma'\ell'}\frac{T_{cb'}(k')[T^*_{c'b'}(k')(1-f_{k'})\phi_{c'b}(k)-(1-f_k)\phi^*_{c'b'}(k')T_{c'b}(k)]}{E_k-E_{k'}-(E_{b'}-E_b)+i0^+}$$

$$+\sum_{b',c',k'\sigma'\ell'}\frac{[f_{k'}\phi_{cb'}(k)T^*_{c'b'}(k')-T_{cb'}(k)f_k\phi^*_{c'b'}(k')]T_{c'b}(k')}{E_k-E_{k'}-(E_c-E_{c'})+i0^+}$$

$$+\sum_{c',d,k'\sigma'\ell'}\frac{[T^*_{dc}(k')(1-f_{k'})\phi_{dc'}(k)-(1-f_k)\phi^*_{dc}(k')T_{dc'}(k)]T_{c'b}(k')}{E_k-E_{k'}-(E_c-E_{c'})+i0^+}$$

$$+\sum_{c',d,k'\sigma'\ell'}\frac{T^*_{dc}(k')[(1-f_{k'})\phi_{dc'}(k)T_{c'b}(k')-T_{dc'}(k)f_k\phi_{c'b}(k')]}{E_k+E_{k'}-(E_d-E_b)+i0^+}$$

$$+\sum_{c',d,k'\sigma'\ell'}\frac{T^*_{dc}(k')[T_{dc'}(k')f_{k'}\phi_{c'b}(k)-(1-f_k)\phi_{dc'}(k')T_{c'b}(k)]}{E_k+E_{k'}-(E_d-E_b)+i0^+}, \tag{10}$$

$$i\hbar\frac{d}{dt}w_{bb'}=(E_b-E_{b'})w_{bb'}+\sum_{a,k\sigma\ell}[T_{ba}(k)\phi^*_{b'a}(k)-\phi_{ba}(k)T^*_{b'a}(k)]+\sum_{c,k\sigma\ell}[T^*_{cb}(k)\phi_{cb'}(k)-\phi^*_{cb}(k)T_{cb'}(k)] \tag{11}$$

These equations are the main result of this paper. They satisfy current conservation, as shown in Appendix C. The numerical implementation of this approach is straightforward and we will give examples in the following sections.

If we entirely neglect the correlated two-particle transitions, only the first line of Eq. (10) remains. Applying the Markov limit we obtain a set of equations analogously to Eqs. (2a,b) of Ref. 18. This shows that our approximation scheme goes substantially beyond the rate equation scheme of Gurvitz,[18] which only holds in the high-bias limit.

III. SINGLE LEVEL WITHOUT SPIN

In order to demonstrate the formalism described in the preceding section we consider a single level without spin. We show that this case can be solved analytically in the stationary state and that the exact nonequilibrium Green function result is recovered.

The possible dot states are the empty state 0 with energy $E_0=0$ and the occupied state 1 with energy E_1. The coupling matrix elements between the leads and the dot are $T_{10}(k\ell)=T_\ell(k)$, and the others equal zero.

Inserting this in Eq. (10) with $c=1$ and $b=0$ gives

$$i\hbar\frac{d}{dt}\phi_{10}(k\ell)=[E_1-E_k+\Sigma(E_k)]\phi_{10}(k\ell)-T_\ell(k)\sum_{k'\ell'}\frac{T_{\ell'}(k')\phi^*_{10}(k'\ell')}{E_k-E'_k+i0^+}+T_\ell(k)(f_k-w_{11}), \tag{12}$$

where the self-energy

$$\Sigma(E)=\sum_{k\ell}\frac{|T_\ell(k)|^2}{E-E_k+i0^+} \tag{13}$$

has been introduced, and we have used the normalization of the probability $w_{00}+w_{11}=1$.

After multiplying Eq. (12) with $T^*_\ell(k)\delta(E-E_k)$ and summing over all k-states (in a fixed lead ℓ) we obtain

$$i\hbar\frac{d}{dt}B^\ell_{10}(E)=[E_1-E+\Sigma(E)]B^\ell_{10}(E)-\frac{\Gamma_\ell(E)}{2\pi}\int dE'\frac{B^{L*}_{10}(E')+B^{R*}_{10}(E')}{E-E'+i0^+}+\frac{\Gamma_\ell(E)}{2\pi}[f_\ell(E)-w_{11}] \tag{14}$$

for the new variable

$$B^\ell_{10}(E)=\sum_k\delta(E-E_k)T^*_\ell(k)\phi_{10}(k\ell), \tag{15}$$

where $\Gamma_\ell(E)=2\pi\Sigma_k\delta(E-E_k)|T_\ell(k)|^2$.

Equation (11) becomes

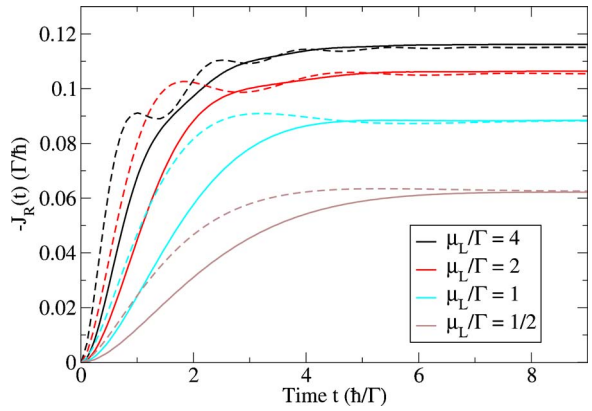

FIG. 1. (Color online) The time-dependent current calculated with our method (full line) and with the time-dependent Green function method from Ref. 21 (dashed line) as response to a steplike modulation of the bias with step height μ_L. The coupling is $\Gamma_L=\Gamma_R=\Gamma/2$, the temperature $k_BT=0.05\Gamma$, and the half-width of the band is $W=30\Gamma$.

$$\frac{d}{dt}w_{11} = -\frac{2}{\hbar}\int dE\ \mathrm{Im}\{B^L_{10}(E) + B^R_{10}(E)\}. \tag{16}$$

Finally, the current formula Eq. (6) yields

$$J_L = -\frac{2}{\hbar}\int dE\ \mathrm{Im}\{B^L_{10}(E)\}. \tag{17}$$

Throughout this paper, we apply Fermi functions $f_{k\sigma\ell}=1/[\exp((E_k-\mu_\ell)/k_BT)+1]\equiv f_\ell(E_k)$ for the lead occupations with chemical potentials μ_ℓ and temperature T. Except for this section, the bias V is applied symmetrically around zero, i.e., $\mu_L=V/2$, $\mu_R=-V/2$. The contact functions $\Gamma_\ell(E)$ are assumed to be zero for $|E|>W$, while they take the constant values Γ_ℓ, independent of spin, for $|E|<0.95W$. For $0.95W<|E|<W$ we interpolate with an elliptic behavior in order to avoid discontinuities.

The time-dependent net-current $J_R(t)$ flowing from the right lead into the single level has been calculated from Eqs. (14), (16), and (17) in the following situation: For times $t<0$ the chemical potentials of both leads and the single level are aligned, i.e., $\mu_L^0=\mu_R^0=E_1=0$. At $t=0$ the chemical potential of the left lead is raised instantaneously to μ_L giving a steplike modulation of the bias. The result is shown for different values of μ_L in Fig. 1. Also shown is the result of an exact time-dependent Green function calculation.[21] It is not surprising that our results do not show the exact time dependence because the Markov limit has been invoked in the derivation of the generalized equation system in Eqs. (10) and (11).

In the long-time limit, we reach a stationary state with the current

$$J_L = J_R = \frac{1}{\hbar}\int \frac{dE}{2\pi}\frac{\Gamma_L(E)\Gamma_R(E)[f_L(E)-f_R(E)]}{|E-E_1-\Sigma(E)|^2}, \tag{18}$$

which is derived analytically in Appendix D. Equation (18) is in full agreement with the exact nonequilibrium Green function result.[8]

IV. DOUBLE QUANTUM DOT

The double quantum dot structure, where the dots are coupled in series, is a standard example to study tunneling through a multiple-level system. In case of Coulomb interaction and finite bias the validity of both the rate equation method and the Green function formalism is limited.

To simplify the analysis we treat the spinless case. (A possible realization is to favor one spin polarization of the electron by a high magnetic field.) Denoting the left/right dot by α/β, the Hamiltonian reads

$$H = E_\alpha d_\alpha^\dagger d_\alpha + E_\beta d_\beta^\dagger d_\beta + U d_\alpha^\dagger d_\alpha d_\beta^\dagger d_\beta + (\Omega d_\beta^\dagger d_\alpha + \mathrm{H.c.}) + \sum_{k\ell} E_{k\ell} c_{k\ell}^\dagger c_{k\ell} + \sum_k (t_{kL} d_\alpha^\dagger c_{kL} + t_{kR} d_\beta^\dagger c_{kR} + \mathrm{H.c.}) \tag{19}$$

with Ω being the interdot tunneling coupling and U the Coulomb energy for occupying both dots. The first four terms describe the isolated double quantum dot H_D. Diagonalizing this part of the Hamiltonian gives the following states:

$$|0\rangle = |0\rangle, \quad E_0 = 0,$$

$$|1\rangle = (\alpha_1 d_\alpha^\dagger + \beta_1 d_\beta^\dagger)|0\rangle, \quad E_1 = \tfrac{1}{2}(\rho - \sqrt{\Delta^2+4\Omega^2}),$$

$$|2\rangle = (\alpha_2 d_\alpha^\dagger + \beta_2 d_\beta^\dagger)|0\rangle, \quad E_2 = \tfrac{1}{2}(\rho + \sqrt{\Delta^2+4\Omega^2}),$$

$$|d\rangle = d_\alpha^\dagger d_\beta^\dagger|0\rangle, \quad E_d = E_\alpha + E_\beta + U,$$

with $\Delta=E_\alpha-E_\beta$, $\rho=E_\alpha+E_\beta$, $C_\pm=(\Delta\pm\sqrt{\Delta^2+4\Omega^2})/2\Omega$, $\alpha_{1/2}=C_\mp/\sqrt{1+C_\mp^2}$, and $\beta_{1/2}=1/\sqrt{1+C_\mp^2}$.

From Appendix A we find

$$H_T = \sum_{k\ell}[T^\ell_{10}(k)|1\rangle\langle 0|c_{k\ell} + T^\ell_{20}(k)|2\rangle\langle 0|c_{k\ell} + T^\ell_{d1}(k)|d\rangle\langle 1|c_{k\ell} + T^\ell_{d2}(k)|d\rangle\langle 2|c_{k\ell}] + \mathrm{H.c.} \tag{20}$$

with (skipping the k-dependence of the matrix elements)

$$T^L_{10} = t^*_L\langle 1|d_\alpha^\dagger|0\rangle = t^*_L\alpha^*_1, \quad T^L_{20} = t^*_L\langle 2|d_\alpha^\dagger|0\rangle = t^*_L\alpha^*_2,$$

$$T^R_{10} = t^*_R\langle 1|d_\beta^\dagger|0\rangle = t^*_R\beta^*_1, \quad T^R_{20} = t^*_R\langle 2|d_\beta^\dagger|0\rangle = t^*_R\beta^*_2,$$

$$T^L_{d1} = t^*_L\langle d|d_\alpha^\dagger|1\rangle = t^*_L\beta_1, \quad T^L_{d2} = t^*_L\langle d|d_\alpha^\dagger|2\rangle = t^*_L\beta_2,$$

$$T^R_{d1} = t^*_R\langle d|d_\beta^\dagger|1\rangle = -t^*_R\alpha_1, \quad T^R_{d2} = t^*_R\langle d|d_\beta^\dagger|2\rangle = -t^*_R\alpha_2,$$

where the signs of the coupling matrix elements are due to the order of the operators in the double-occupied state.

Applying the method in the same way as for the single level system gives eight different functions of the type $B^\ell_{cb}(E)$ and five different occupations $\omega_{bb'}$. These equations have been solved and the stationary current has been recorded.

By comparing with exact Green function results, it has been verified numerically that in the noninteracting case ($U=0$) the exact transmission is obtained for various values of level splitting and interdot coupling (not shown). Furthermore, for both $U=0$ and nonzero U we have calculated the stationary current in a situation where the levels are

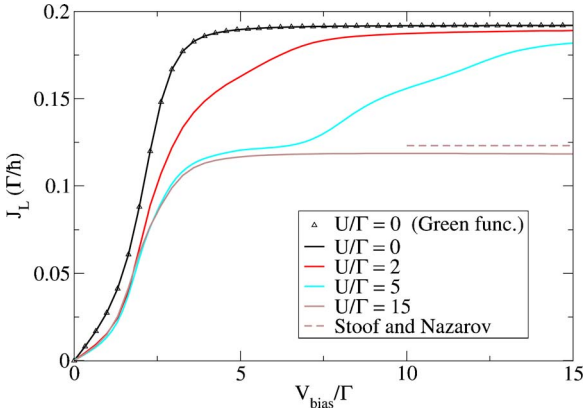

FIG. 2. (Color online) Stationary current through the double quantum dot structure for different values of the interdot Coulomb repulsion U. The triangles are from a nonequilibrium Green function calculation, and the dotted line is the result by Stoof and Nazarov (Ref. 22) valid in high-bias limit for $U\to\infty$. The levels of the dot are placed symmetrically around the zero-bias with $E_\alpha - E_\beta = \Gamma$. We use the interdot tunneling coupling $\Omega=\Gamma$, $\Gamma_L=\Gamma_R=\Gamma/2$, the temperature $k_BT=0.1\Gamma$, and the half-width of the band $W=20\Gamma$.

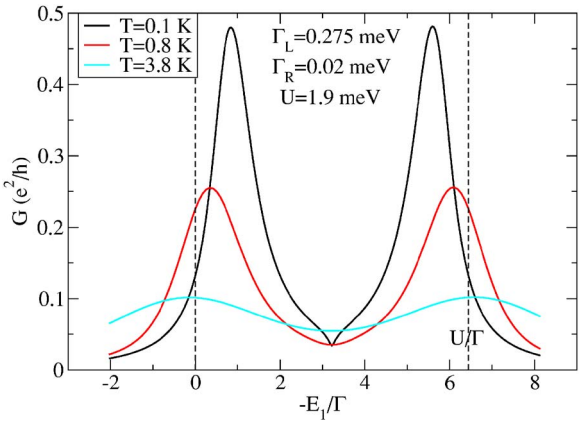

FIG. 3. (Color online) Zero-bias conductance as a function of level position for different temperatures. All parameters are according to the experimental data shown in Fig. 2 of Ref. 23.

dealigned with $E_\alpha=-E_\beta=0.5\Gamma$, and $\Omega=\Gamma$. The results for different values of U are shown in Fig. 2 together with the Green function result for $U=0$. Obviously, the latter is fully recovered in the noninteracting limit. The straight dashed line in the figure is the quantum rate equation result obtained by Stoof and Nazarov,[22] which is valid in the high-bias limit ($V\to\infty$) for $U\to\infty$. The same result is found in Ref. 7 using another rate equation method. The small discrepancy between the results could be due to the finite bandwidth used in our calculation. For intermediate values of U the results looks reasonable and exhibit a smooth interpolation between the limiting cases. The kink on the curve for finite U is due to the single occupied state.

V. SPIN-DEGENERATE LEVEL

Now we consider a spin-degenerate single level with energy E_1 and Coulomb interaction U. We use the parameters $U=1.9$ meV, and $\Gamma=\Gamma_L+\Gamma_R=0.295$ meV, as experimentally determined for the structure studied in Ref. 23. The conductance

$$G = e^2\frac{dJ}{d(\mu_L-\mu_R)} \tag{21}$$

is expected to reach $G_0=(e^2/h)8\Gamma_L\Gamma_R/(\Gamma_L+\Gamma_R)^2$ in the zero-bias limit $\mu_L\to\mu_R$ for temperatures far below the Kondo temperature T_K.[24,25] As $G_{\max}\approx 0.5e^2/h$ in the experiment we use $\Gamma_L=0.275$ meV and $\Gamma_R=0.02$ meV. Furthermore the band width $W=5$ meV is applied. In Fig. 3 we show the zero-bias conductance as a function of the dot level, which is modified by a gate bias in the experiment. We find the standard Coulomb oscillations, where the conductance exhibits peaks whenever the single-particle excitation energies are close to the Fermi edge of the contacts, $\mu=0$ (depicted by vertical dashed lines at $E_1=0$ and $E_1=-U$). The peak positions and widths are in good agreement with the data given in Fig. 2 of Ref. 23. The peak heights for the peak around $E_1\approx 0$ agree reasonably with the experiment, if one takes into account that for elevated temperatures the presence of different levels raise the conductance which is not included in our single-level model. (The experimental level spacing corresponds to 5 K.) The experimental peak heights for the peak at $E_1\approx -U$ are lower, while they are exactly identical with the corresponding peaks $E_1\approx 0$ due to electron-hole symmetry in our calculation. Possible sources for this deviation result from an energy-dependence of the $\Gamma_\ell(E)$ in the experiment or the admixture of different levels.

Further lowering the temperature, the zero-bias conductance should increase in the region $0<E_1<U$, due to the Kondo effect.[24,25] Albeit we observe an increase in parts of this region, the (probable unphysical) dip in our curve for $T=0.1$K at $E_1=-U/2$ persists even at lower temperatures. Furthermore the conductance can exceed G_0 at the peaks. This indicates that our approach fails in the Kondo limit, where strong correlations between lead and dot state require elaborated renormalization group[26–28] or slave boson[29,30] techniques.

In Fig. 4 we show the finite bias conductance at 0.8 K, where both the conductance peaks for $\mu_L\approx\mu_R$ discussed

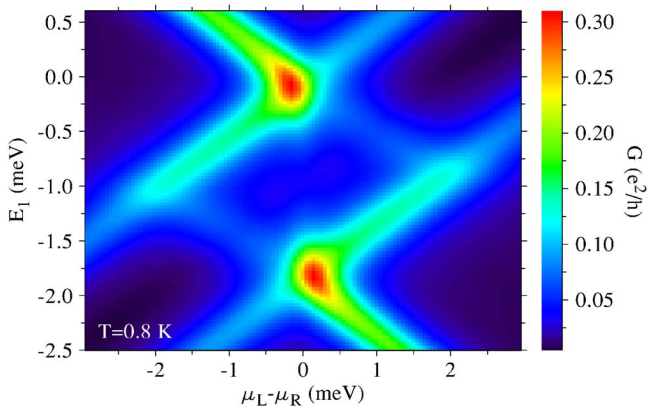

FIG. 4. (Color online) Differential conductance for finite bias. Parameters as in Fig. 3.

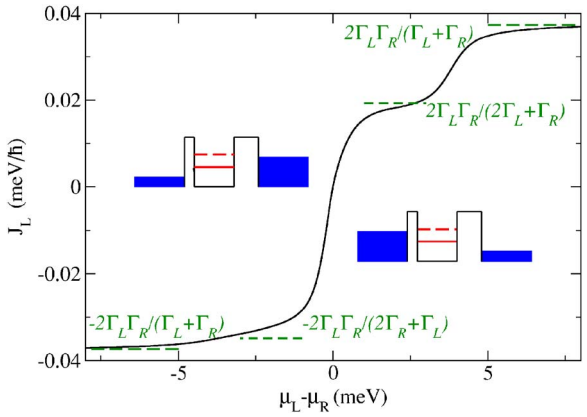

FIG. 5. (Color online) Current versus bias for $E_1=0$ and $T=0.8$ K. Parameters as in Fig. 3. The dashed horizontal lines correspond to the rate equation model by Gurvitz and Prager (Ref. 7), where we added the respective formulas.

above as well as the excitations can be detected. We observe a strong asymmetry due to $\Gamma_L \gg \Gamma_R$. This can be understood from Fig. 5, where the current is plotted versus bias at the single-electron excitation peak $E_1=0$. For negative bias the electrons rapidly leave the dot via the thin left barrier and the dot is essentially empty. Thus both spin directions can tunnel through the thick right barrier, which is limiting the current. In contrast, for positive bias the dot is occupied with a single electron (as long as $\mu_L=V/2<E_1+U$) with a given spin and only this spin direction may tunnel through the thick barrier, reducing the current approximately by a factor of 2. We have shown the respective results for the rate equation model[7] for comparison. The short-dashed horizontal lines refer to a bias which allows only single occupation of the dot, while the long-dashed line considers the case where both the single- and the two-particle state are located between both Fermi levels. The currents from the rate equation model slightly exceed our results, as the peaks are not completely within the bias window due to broadening.

VI. DISCUSSION AND SUMMARY

We have presented an approach for transport through finite systems based on the Liouville equation. This approach recovers the results from the Green-function method in the noninteracting limit for the models studied. In the high-bias limit the results are consistent with the many-particle rate equations. Thus it bridges the gap between these approaches and allows for a consistent treatment of Coulomb interaction and broadening effects for arbitrary bias. For example, Coulomb blockade peaks are correctly reproduced. The model fails below the Kondo temperature where strong correlations between the finite system and the contacts dominate the behavior.

Correlations between tunneling events have been previously studied by the method of a diagrammatic real-time technique.[31] While this work was completed we also became aware of a cumulant expansion of the tunneling Hamiltonian.[32] It would be interesting to study the relation between these approaches and our method. A central question is here, whether the exact Green function result, such as Eq. (18), can be obtained for the noninteracting case.

The numerical implementation of our approach is straightforward and explicit results were presented for standard model systems made by up to two single-particle states. For larger systems the number of many-particle states b,c increases dramatically, and so does the number of ϕ_{bc} functions. Thus sophisticated routines are needed for the implementation and evaluation of real systems.

ACKNOWLEDGMENTS

The authors thank J. Paaske for helpful discussions regarding the Kondo effect. This work was supported by the Swedish Research Council (VR).

APPENDIX A: DETERMINATION OF MATRIX ELEMENTS $T_{ab}(k)$

Conventually one starts with a single-particle basis in the central region with wave functions $\Psi_n(\mathbf{r})$, spin functions χ_σ and associated creation operators $d^\dagger_{n\sigma}$. Then an arbitrary many-particle state $|a\rangle$ can be written as

$$|a\rangle = \sum_{\mathbf{j}} a_{\mathbf{j}} d^\dagger_{j_1} d^\dagger_{j_2} \cdots d^\dagger_{j_{N_a}} |0\rangle,$$

where $j_i=n_i\sigma_i$ determines the ith single-particle state in the N_a-particle Slater determinant determined by the index set $\mathbf{j}=(j_1,j_2,\ldots,j_{N_a})$. In order to avoid double counting, we restrict to the ordering $n_1\leqslant n_2\leqslant\cdots\leqslant n_{N_a}$, where spin-up precedes spin-down for equal n. The expansion coefficients $a_{\mathbf{j}}$ can be obtained by exact diagonalization of the dot Hamiltonian.

In the single-particle basis the tunneling Hamiltonian reads

$$H_T = \sum_{k\sigma\ell,n} (t^*_{n\ell}(k\sigma\ell) c^\dagger_{k\sigma\ell} d_{n\sigma} + t_{n\ell}(k\sigma\ell) d^\dagger_{n\sigma} c_{k\sigma\ell}). \quad \text{(A1)}$$

Inserting the unit operators $\Sigma_a |a\rangle\langle a|$, $\Sigma_b |b\rangle\langle b|$ we find

$$H_T = \sum_{k\sigma\ell,a,b} \Bigg(c^\dagger_{k\sigma\ell}|b\rangle \underbrace{\sum_n t^*_{n\ell}(k\sigma\ell)\langle b|d_{n\sigma}|a\rangle}_{=T^*_{ab}(k\sigma\ell)} \langle a| + |a\rangle \underbrace{\sum_n t_{n\ell}(k\sigma\ell)\langle a|d^\dagger_{n\sigma}|b\rangle}_{=T_{ab}(k\sigma\ell)} \langle b| c_{k\sigma\ell} \Bigg) \quad \text{(A2)}$$

to be used in Eq. (4).

APPENDIX B: DERIVATION OF EQS. (10) AND (11)

Using the approximation (i) we find for one of the two-electron transition terms in Eq. (7),

$$i\hbar\frac{d}{dt}\rho_{b'g-k\sigma\ell+k'\sigma'\ell';bg} = (E_{b'} + E_{k'} - E_b - E_k)\rho_{b'g-k+k';bg} - \sum_a T_{b'a}(k)\rho_{agk+k';bg} + \sum_{c'} T^*_{c'b'}(k')\rho_{c'g-k\bar{k}';bg} - \sum_{c'} \rho_{b'g-k+k';c'g-k}T_{c'b}(k) - \sum_a \rho_{b'g-k+k';ag+k'}T^*_{ba}(k').$$

Now we take the Markov limit (ii) following the standard treatment of density matrix theory for ultrafast dynamics.[20] This implies adding $-i0^+\rho_{b'g-k\sigma\ell+k'\sigma'\ell';bg}$ on the right-hand side in order to guarantee the decay of initial conditions at $t=-\infty$, and neglecting the time dependence of the inhomogeneity[33] (second and third line). Then this linear differential equation can be solved directly, yielding

$$\rho_{b'g-k\sigma\ell+k'\sigma'\ell';bg} = \frac{1}{E_k - E_{k'} - (E_{b'} - E_b) + i0^+} \times \Big(- \sum_a T_{b'a}(k)\rho_{agk+k';bg} + \sum_{c'} T^*_{c'b'}(k')\rho_{c'g-k\bar{k}';bg} - \sum_{c'} \rho_{b'g-k+k';c'g-k}T_{c'b}(k) - \sum_a \rho_{b'g-k+k';ag+k'}T^*_{ba}(k') \Big).$$

In the same way the other two-electron transition terms in Eq. (7) are determined by

$$\rho_{dg-k\sigma\ell-k'\sigma'\ell';bg} = \frac{1}{E_k + E_{k'} - (E_d - E_b) + i0^+} \times \sum_{c'} (-T_{dc'}(k)\rho_{c'gk-k';bg} + T_{dc'}(k')\rho_{c'g-kk';bg} - \rho_{dg-k-k';c'g-k}T_{c'b}(k) - \rho_{dg-k-k';c'g-k'}T_{c'b}(k')),$$

$$\rho_{cg-k\sigma\ell;c'g-k'\sigma'\ell'} = \frac{1}{E_k - E_{k'} - (E_c - E_{c'}) + i0^+} \times \Big(\sum_{b'} T_{cb'}(k)\rho_{b'gk;c'g-k'} + \sum_d T^*_{dc}(k')\rho_{dg-k-k';c'g-k'} - \sum_d \rho_{cg-k;dg-k'-k}T_{dc'}(k) - \sum_{b'} \rho_{cg-k;b'gk'}T^*_{c'b'}(k') \Big),$$

$$\rho_{cg-k\sigma\ell;ag+k'\sigma'\ell'} = \frac{1}{E_k + E_{k'} - (E_c - E_a) + i0^+} \times \sum_{b'} [T_{cb'}(k)\rho_{b'gk;ag+k'} + T_{cb'}(k')\rho_{b'g-k+k';ag+k'} - \rho_{cg-k;b'g+k'-k}T_{b'a}(k) - \rho_{cg-k;b'g\bar{k}'}T_{b'a}(k')].$$

In order to obtain Eq. (10) we sum over g in Eq. (7) after inserting the above approximations for the two-electron transition terms. Using the definitions (8) and (9) and the decoupling assumption (iii) we obtain

$$\sum_g \rho_{b'gk;bg} = \sum_g \delta_{N_k,1}\rho_{b'g;bg} \approx f_k \sum_g \rho_{b'g;bg} = f_k w_{b'b}.$$

Similarly

$$\sum_g \rho_{b'g\bar{k};bg} \approx (1 - f_k)w_{b'b},$$

$$\sum_g \rho_{bg-k'k;ag} \approx f_k \phi_{ba}(k'),$$

$$\sum_g \rho_{bg-k'\bar{k};ag} \approx (1 - f_k)\phi_{ba}(k').$$

Furthermore note that

$$\sum_g \rho_{bg;ag+k} = \sum_{\tilde{g}} \rho_{b\tilde{g}-k;a\tilde{g}} = \phi_{ba}(k),$$

$$\sum_g \rho_{b'g+k;bg+k} = \sum_{\tilde{g}} \rho_{b'\tilde{g}k;b\tilde{g}} \approx f_k w_{b'b},$$

as well as similar relations hold, where $|\tilde{g}\rangle$ is identical with $|g\rangle$ except for exchanging 1 and 0 in the occupation of state k (including the appropriate change of sign). Particular care must be taken in order to insure the anticommutation rules. For example, $\Sigma_g \rho_{b'g-k+k';ag+k'} \approx -f_{k'}\phi_{b'a}(k)$.

In the same way

$$i\hbar\frac{d}{dt}\rho_{bg;b'g} = (E_b - E_{b'})\rho_{bg;b'g} + \sum_{a,k\sigma\ell} T_{ba}(k)\rho_{ag+k;b'g} + \sum_{c,k\sigma\ell} T^*_{cb}(k)\rho_{cg-k;b'g} - \sum_{c,k\sigma\ell} \rho_{bg;cg-k}T_{cb'}(k) - \sum_{a,k\sigma\ell} \rho_{bg;ag+k}T^*_{b'a}(k).$$

gives Eq. (11) after summing over g.

APPENDIX C: CONSERVATION OF CURRENT

We will in the following show that the formalism obeys current conservation, i.e.,

$$\frac{d}{dt}\langle \hat{N}_D \rangle = J_L + J_R, \tag{C1}$$

with $\hat{N}_D = \Sigma_b N_b |b\rangle\langle b|$ being the number operator of the dot. From the definition of the density operator we get

$$\frac{d}{dt}\langle \hat{N}_D\rangle = \frac{d}{dt}\mathrm{Tr}(\rho \hat{N}_D) = \sum_b N_b \frac{d}{dt} w_{bb}. \tag{C2}$$

The time derivative of w_{bb} is obtained from Eq. (11)

$$\frac{d}{dt} w_{bb} = -\frac{2}{\hbar}\sum_{ak\sigma\ell} \mathrm{Im}\{T^*_{ba}(k)\phi_{ba}(k)\} + \frac{2}{\hbar}\sum_{ck\sigma\ell} \mathrm{Im}\{T^*_{cb}(k)\phi_{cb}(k)\}. \tag{C3}$$

Inserting this in Eq. (C2) and renaming the summation indices in the second term leads to

$$\frac{d}{dt}\langle \hat{N}_D\rangle = -\frac{2}{\hbar}\sum_{bak\sigma\ell} (N_b - N_a)\mathrm{Im}\{T^*_{ba}(k)\phi_{ba}(k)\}. \tag{C4}$$

Now the $T_{ba}(k)$-matrix elements are vanishing for $N_b \neq N_a + 1$, and the right-hand side of Eq. (C4) becomes $J_L + J_R$ using the definition of the currents Eq. (6). Thus, current conservation (C1) holds.

APPENDIX D: DERIVATION OF EQ. (18)

Defining $B_{10} = B^L_{10} + B^R_{10}$ and $\Gamma = \Gamma^L + \Gamma^R$ we find from Eq. (14),

$$\begin{aligned} i\hbar \frac{d}{dt} B_{10}(E) = {} & [E_1 - E + \mathrm{Re}\{\Sigma(E)\}]B_{10}(E) + \Gamma(E)\mathrm{Im}\{B_{10}(E)\} \\ & - \frac{\Gamma(E)}{2\pi}\int dE' \mathcal{P}\left\{\frac{B^*_{10}(E')}{E - E'}\right\} \\ & + \frac{\Gamma_L(E) f_L(E) + \Gamma_R(E) f_R(E)}{2\pi} - w_{11}\frac{\Gamma(E)}{2\pi}, \end{aligned} \tag{D1}$$

where $\mathrm{Im}\{\Sigma(E)\} = -\Gamma(E)/2$ has been used. Equation (D1) is a linear inhomogeneous differential equation which has a particular stationary real solution $B^{\mathrm{stat}}_{10}(E)$ determined by

$$\begin{aligned} & \frac{\Gamma(E)}{2\pi}\int dE' \mathcal{P}\left\{\frac{B^{\mathrm{stat}}_{10}(E')}{E - E'}\right\} \\ & \quad = [E_1 - E + \mathrm{Re}\{\Sigma(E)\}]B^{\mathrm{stat}}_{10}(E) \\ & \qquad + \frac{\Gamma_L(E) f_L(E) + \Gamma_R(E) f_R(E)}{2\pi} - w_{11}\frac{\Gamma(E)}{2\pi}. \end{aligned} \tag{D2}$$

Numerically, we find that this solution is indeed reached from different initial conditions in the long-time limit. Inserting the integral over $B^{\mathrm{stat}}_{10}(E)$ from Eq. (D2) into Eq. (14) gives the stationary solution

$$\begin{aligned} [E_1 - E + \Sigma(E)]B^L_{10}(E) = {} & \Gamma_L(E)\frac{E_1 - E + \Sigma(E)}{\Gamma(E)} B^{\mathrm{stat}}_{10}(E) \\ & + \frac{\Gamma_L(E)\Gamma_R(E)[f_R(E) - f_L(E)]}{2\pi\Gamma(E)}. \end{aligned} \tag{D3}$$

As $B^{\mathrm{stat}}_{10}(E)$ is real it does not contribute to the imaginary part of $B^L_{10}(E)$ in Eq. (17) providing the final result (18).

[1] S. Datta, *Electronic Transport in Mesoscopic Systems* (Cambridge University Press, Cambridge, 1995).
[2] D. K. Ferry and S. M. Goodnick, *Transport in Nanostructures* (Cambridge University Press, Cambridge, 1997).
[3] Y. Imry, *Introduction to Mesoscopic Physics* (Oxford University Press, Oxford, 2001).
[4] C. W. J. Beenakker, Phys. Rev. B **44**, 1646 (1991).
[5] J. M. Kinaret, Y. Meir, N. S. Wingreen, P. A. Lee, and X. G. Wen, Phys. Rev. B **46**, 4681 (1992).
[6] D. Pfannkuche and S. E. Ulloa, Phys. Rev. Lett. **74**, 1194 (1995).
[7] S. A. Gurvitz and Y. S. Prager, Phys. Rev. B **53**, 15932 (1996).
[8] Y. Meir and N. S. Wingreen, Phys. Rev. Lett. **68**, 2512 (1992).
[9] H. Haug and A.-P. Jauho, *Quantum Kinetics in Transport and Optics of Semiconductors* (Springer, Berlin, 1996).
[10] W. R. Frensley, Rev. Mod. Phys. **62**, 745 (1990).
[11] M. Di Ventra and N. D. Lang, Phys. Rev. B **65**, 045402 (2002).
[12] M. Brandbyge, J.-L. Mozos, P. Ordejón, J. Taylor, and K. Stokbro, Phys. Rev. B **65**, 165401 (2002).
[13] Y. Xue, S. Datta, and M. A. Ratner, Chem. Phys. **281**, 151 (2002).
[14] P. Havu, V. Havu, M. J. Puska, and R. M. Nieminen, Phys. Rev. B **69**, 115325 (2004).
[15] W. Pötz, J. Appl. Phys. **66**, 2458 (1989).
[16] S. E. Laux, A. Kumar, and M. V. Fischetti, J. Appl. Phys. **95**, 5545 (2004).
[17] H. Sprekeler, G. Kießlich, A. Wacker, and E. Schöll, Phys. Rev. B **69**, 125328 (2004).
[18] S. A. Gurvitz, Phys. Rev. B **57**, 6602 (1998).
[19] A. Wacker, in *Advances in Solid State Phyics*, edited by B. Kramer (Springer, Berlin, 2001), p. 199.
[20] T. Kuhn, in *Theory of Transport Properties of Semiconductor Nanostructures*, edited by E. Schöll (Chapman and Hall, London, 1998).
[21] G. Stefanucci and C.-O. Almbladh, Phys. Rev. B **69**, 195318 (2004).
[22] T. H. Stoof and Y. V. Nazarov, Phys. Rev. B **53**, 1050 (1996).
[23] D. Goldhaber-Gordon, J. Göres, M. A. Kastner, H. Shtrikman, D. Mahalu, and U. Meirav, Phys. Rev. Lett. **81**, 5225 (1998).
[24] T. K. Ng and P. A. Lee, Phys. Rev. Lett. **61**, 1768 (1988).
[25] L. I. Glazman and M. E. Raikh, JETP Lett. **47**, 452 (1988).
[26] T. A. Costi, A. C. Hewson, and V. Zlatić, J. Phys.: Condens. Matter **6**, 2519 (1994).
[27] H. Schoeller and J. König, Phys. Rev. Lett. **84**, 3686 (2000).
[28] A. Rosch, J. Paaske, J. Kroha, and P. Wölfle, Phys. Rev. Lett. **90**, 076804 (2003).
[29] N. S. Wingreen and Y. Meir, Phys. Rev. B **49**, 11040 (1994).

[30] B. Dong and X. L. Lei, J. Phys.: Condens. Matter **13**, 9245 (2001).
[31] J. König, H. Schoeller, and G. Schön, Phys. Rev. Lett. **78**, 4482 (1997).
[32] X.-Q. Li, J. Luo, Y.-G. Yang, P. Cui, and Y. J. Yan, Phys. Rev. B **71**, 205304 (2005).
[33] This becomes exact for the stationary state, but can, however, produce incorrect results for the time dependence.